AIAA Journal
Vol. 44, No. 6, June 2006

Technical Notes

TECHNICAL NOTES are short manuscripts describing new developments or important results of a preliminary nature. These Notes should not exceed 2500 words (where a figure or table counts as 200 words). Following informal review by the Editors, they may be published within a few months of the date of receipt. Style requirements are the same as for regular contributions (see inside back cover).

Impact of Subgrid-Scale Models on Jet Turbulence and Noise

Ali Uzun,* Gregory A. Blaisdell,† and Anastasios S. Lyrintzis‡
Purdue University, West Lafayette, Indiana 47907

Introduction

VISBAL and Rizzetta[1] and Visbal et al.[2] have recently performed large-eddy simulation (LES) calculations of turbulent channel flow and compressible isotropic turbulence decay without using any explicit subgrid-scale (SGS) model. In those simulations, spatial filtering was treated as an implicit SGS model. They also showed that use of an SGS model in those simulations did not produce results superior to those obtained without employing an SGS model. Bogey and Bailly[3] also performed LES calculations for jet flows by using spatial filtering only. Moreover, they brought up the issue of the effects of the eddy–viscosity-based Smagorinsky SGS model on jet noise in yet another recent study.[4,5] They showed that the high-frequency portion of the noise spectra was significantly suppressed by the eddy–viscosity. It is well understood that in turbulent flows the energy cascade is associated with a mean flux of energy that is directed from large scales toward small scales. The large scales contain the major part of the turbulent kinetic energy, and they continuously feed the turbulent kinetic energy via the cascade to the smallest eddies where it is dissipated. Because the grid resolution is too coarse to resolve all of the relevant length scales in an LES, the pile-up of energy at high wave numbers can be eliminated through the use of a spatial filter. Hence, the spatial filter can be thought of as an effective SGS model in an LES. In this study, we perform two jet simulations to study the impact of the SGS model on jet turbulence and far-field noise. The first simulation does not employ any explicit SGS model, but treats the spatial filter as an implicit SGS model. In the second simulation, we employ a localized version of the dynamic Smagorinsky model (DSM) (see Ref. 6) and keep all test case parameters the same as those in the first simulation. We examine the differences between the two simulations to quantify the effect of the SGS model on the near-field jet turbulence and the far-field noise. Although this study is similar to those done by Bogey and Bailly,[4,5] our work additionally does a comparison of the two LES results with experimental jet noise spectra with the hope of shedding some light on which type of LES is better. Moreover, our simulations resolve frequencies up to Strouhal number three, which is higher than the Strouhal number two maximum frequency that was resolved in Bogey and Bailly's calculations.[3–5]

Received 26 March 2004; revision received 2 February 2006; accepted for publication 14 March 2006.

*Graduate Research Assistant, School of Aeronautics and Astronautics; currently Postdoctoral Research Associate, School of Computational Science, Florida State University, Tallahassee, FL 32306. Senior Member AIAA.

†Associate Professor, School of Aeronautics and Astronautics. Senior Member AIAA.

‡Professor, School of Aeronautics and Astronautics. Associate Fellow AIAA.

Governing Equations

The governing equations for LES are obtained by applying a spatial filter to the Navier–Stokes equations to remove the small scales. The explicit SGS model implemented into the code is a localized version of the DSM for compressible flows proposed by Moin et al.[6] The Favre-filtered unsteady, compressible, nondimensionalized Navier–Stokes equations formulated in curvilinear coordinates (see Ref. 7) are solved in this study using the numerical methods described in the next section.

Numerical Methods

We first transform a given nonuniformly spaced curvilinear computational grid in physical space to a uniform grid in computational space and solve the discretized governing equations on the uniform grid. To compute the spatial derivatives at interior grid points away from the boundaries, we employ the nondissipative sixth-order compact scheme developed by Lele.[8] For the left boundary and the right boundary we apply a third-order one-sided compact scheme, and for the points next to the boundaries we use a fourth-order central compact scheme formulation. To stabilize the calculations, we employ a sixth-order tridiagonal spatial filter used by Visbal and Gaitonde.[9] For the dynamic SGS model, a 15-point explicit filter developed by Bogey and Bailly[10] is used as the test filter. In our implementation, the dynamically computed model coefficients are locally averaged in space over three grid points in each direction to avoid sharp fluctuations in the model coefficient. No negative model coefficients are allowed. The upper limit for the model coefficients is set to 0.5. This procedure works reasonably well for the jet flows we are studying.[11] By turning off the localized dynamic Smagorinsky SGS model, we can treat the spatial filter as an implicit SGS model. The standard fourth-order explicit Runge–Kutta scheme is used for time advancement. We apply Tam and Dong's three-dimensional radiation and outflow boundary conditions (see Ref. 12) on the boundaries of the computational domain. We additionally use the sponge zone method[13] in which grid stretching and artificial damping are applied to dissipate the vortices present in the flowfield before they hit the outflow boundary. This way, unwanted reflections from the outflow boundary are suppressed. Because the actual nozzle geometry is not included in the present calculations, randomized perturbations in the form of a vortex ring are added to the velocity profile at a short distance downstream of the inflow boundary to excite the three-dimensional instabilities in the jet and cause the potential core of the jet to break up at a reasonable distance downstream of the inflow boundary. This forcing procedure has been adapted from the work of Bogey et al.[14] More detailed information about the numerical methods employed in the LES code can be found in Ref. 7.

Results

We will present results from LES for a turbulent isothermal round jet at a Mach number of 0.9 and Reynolds number of 4×10^5 that is based on the jet diameter. The jet centerline temperature was chosen to be the same as the ambient temperature and set to 286 K. A fully curvilinear grid consisting of approximately 16 million grid points ($N_x \times N_y \times N_z = 390 \times 200 \times 200$) was used in the simulation. This test case corresponds to one of the test cases studied by Bogey and Bailly.[3] The physical portion of the domain in this simulation extended to 35 jet radii in the streamwise direction and ± 15 jet radii in the transverse directions. A top-hat mean streamwise velocity profile defined by a hyperbolic tangent function was imposed on the inflow boundary. There are about 14 grid points in the initial jet shear layer.

The first LES was done without an explicit SGS model, and the tridiagonal spatial filter was treated as an implicit SGS model. The filtering parameter was set to $\alpha_f = 0.47$. The second simulation was performed by employing the DSM in the LES. Spatial filtering is also employed in this case to remove the very-high-frequency spurious oscillations not supported by the grid resolution. With the DSM model turned on, the LES code required about 50% more computing time than the preceding LES done with filtering only.

In a recent study, Bogey and Bailly[3] took a close look at the effects of the inflow conditions on jet flow and noise. They found out that removing the first 4 of 16 azimuthal forcing modes resulted in noticeably reduced noise levels. Based on their findings, we decided to use this inflow forcing found by Bogey and Bailly[3] to match the available experimental overall sound pressure levels best. The forcing parameter α is set to 0.007.

The peak of the streamwise velocity fluctuations along the jet centerline is reached at around $x = 17.5r_o$ (where r_o is the jet nozzle radius) in both simulations. Figure 1 shows a comparison of the temporal spectra of the streamwise velocity fluctuations at this location. The spectra are plotted as the power spectral density of the streamwise velocity fluctuation u' vs the Strouhal number, which is defined as $Sr = fD_j/U_o$, where f is the frequency and D_j and U_o are the jet nozzle diameter and the jet centerline velocity at the nozzle exit, respectively. As can be seen from the spectra comparison, the low frequencies that correspond to the large scales of turbulent motions are more energetic in the simulation done with the DSM. The higher frequencies that correspond to the finer scales, however, are more energetic in the simulation done without an SGS model. The finer scales in the simulation done with the DSM are less hungry compared to the finer scales in the simulation done without an SGS model. Hence, the portion of the turbulent kinetic energy drained from the large scales toward the finer scales in the simulation done with the DSM is smaller than that in the simulation done without an SGS model. Consequently, there is more turbulent kinetic energy residing in the large scales when the eddy–viscosity-based SGS model is employed in the LES. Admittedly, the mechanism provided here is a speculation at this point because we have not really proved its existence. Other mechanisms may be possible. Also note that the way the turbulent kinetic energy is dissipated is quite different in the two simulations. The filtering procedure eliminates only the spurious fluctuations that are not well resolved by the local grid spacing. In other words, filtering does not affect the well-resolved scales. On the other hand, the eddy–viscosity of the Smagorinsky model dissipates energy over the well-resolved scales near the grid cutoff, as well as the larger, more energetic scales. More specifically, the eddy–viscosity causes the resolved small scales near the grid cutoff to diffuse rapidly, whereas it has a somewhat less severe effect on the larger scales.

It is also of interest to look at the effects of the SGS model on the noise. During the simulations, aeroacoustic data were gathered on an open control surface that starts one jet radius downstream of the inflow boundary and extends to $31r_o$ in the downstream direction. Far-field noise computations were done by supplying the data gathered on the control surface to the Ffowcs Williams–Hawkings method (see Ref. 15). Comparison of the acoustic pressure spectra obtained from the two simulations at the observation angles of $\theta = 30, 45$, and 60 deg (θ being measured from the horizontal downstream of the jet) on a far-field arc at 60 jet radii are presented in Figs. 2–4. The acoustic pressure spectra are plotted as the sound pressure level (SPL) vs the Strouhal number. Figures 2–4 also show a comparison of the LES far-field noise spectra with the experimental noise spectra of a Mach 0.9 isothermal jet studied by Tanna et al.[16] Because the LES spectra are considerably louder than the experimental spectra due to the mismatch of LES inflow conditions and the actual experimental inflow conditions, the experimental spectra are shifted upward in Figs. 2–4 for the sake of making a better

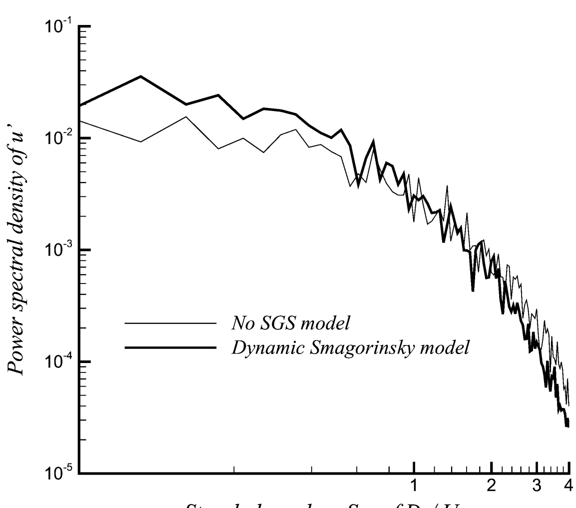

Fig. 1 Temporal spectrum of streamwise velocity fluctuations at $x = 17.5\ r_o$ location on jet centerline.

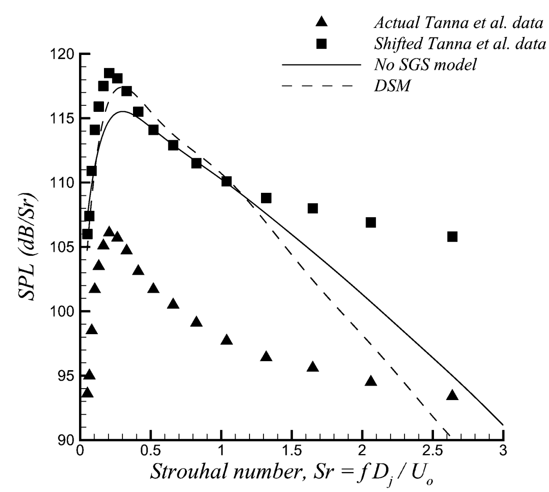

Fig. 2 Acoustic pressure spectra predictions at $R = 60r_o$, $\theta = 30$ deg location on far-field arc and comparison with experiment.

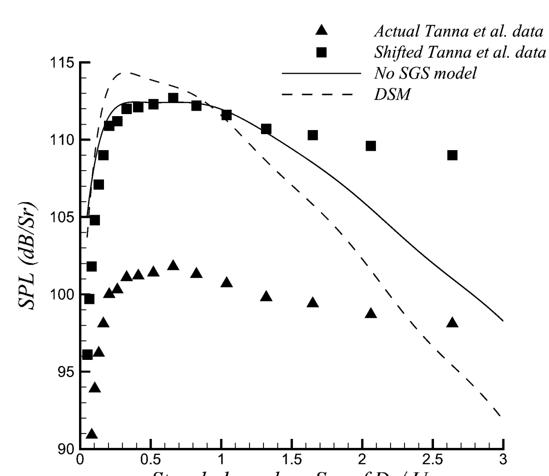

Fig. 3 Acoustic pressure spectra predictions at $R = 60r_o$, $\theta = 45$ deg location on far-field arc and comparison with experiment.

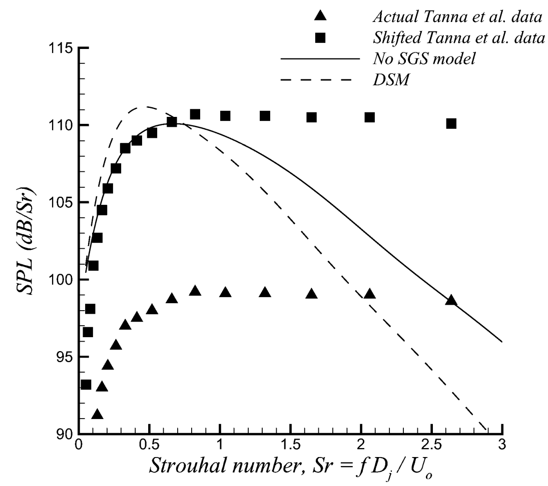

Fig. 4 Acoustic pressure spectra predictions at $R = 60r_o$, $\theta = 60$ deg location on far-field arc and comparison with experiment.

comparison of the spectral shapes. Figures 2–4 also show plots of the actual SPL values of the experimental spectra to demonstrate how much SPL difference exists between the LES and the experiment. As can be seen from Fig. 2, the spectral shapes from both LES at the 30-deg observation angle compare reasonably well with the experimental LES until a Strouhal number of about 1.3. However, the spectrum from the LES done with the DSM seems to be capturing the lower frequencies better (but not the high frequencies) at this observation angle. At the observation angle of 45 deg shown in Fig. 3, we now see that the spectrum shape from the LES with filtering only clearly matches the experimental one fairly well until Strouhal number 1.3. The peak frequency is captured by the LES with filtering only at this observation angle. At the observation angle of 60 deg shown in Fig. 4, the spectrum shape from the LES with filtering only once again matches the experimental one well until Strouhal number of about 0.7. However, the almost flat portion of the experimental spectrum located right after the peak frequency is missed by the LES. The spectral shape comparison at the 90-deg location is similar to the one at 60 deg, and is not included herein for brevity. The decay of both LES spectra in the high-frequency portion of all spectra plots takes place at a faster rate than that observed in the experiment. The differences observed between the numerical and experimental noise spectra in the high-frequency portions of the spectra might be due to various reasons. One reason could be the mismatch of the inflow conditions in the numerical simulations with those in the actual experiment. The experiment was performed at a high enough Reynolds number so that the jet shear layers at the nozzle exit were fully turbulent. In the numerical simulations, because it was deemed computationally too expensive to include the nozzle geometry, laminar shear layers were fed into the domain and randomized velocity fluctuations in the form of a vortex ring were imposed on the jet shear layers. Moreover, it has been observed experimentally[17,18] that high-frequency sources are located a small distance downstream of the jet nozzle, and a significant portion of the noise spectrum originates from this near field of the jet. Hence, the high-frequency noise generated in the near-nozzle jet shear layer within a few diameters downstream of the nozzle exit is missing in the current simulations. The absence of the noise generated just downstream of the nozzle could be responsible for the faster decay rates in the high-frequency range of the spectra in the current computations.

Conclusions

The effects of the SGS model on noise predictions have been shown. The main conclusion from this study is that the jet noise is sensitive to the SGS model. When the DSM is employed in an LES, the spectral energy in the high-frequency part of the noise spectra is significantly reduced due to the eddy–viscosity, whereas there is an increase in low-frequency noise. LES with filtering only, on the other hand, predicts increased spectral energy levels at the higher frequencies and decreased spectral energy levels at the lower frequencies. Our comparisons with experiments seem to indicate that at the 30-deg observation angle, the LES with the DSM seems to produce more accurate results for the low frequencies, whereas, on the other hand, at the 45-deg observation angle, the LES with filtering only produces significantly better results for all frequencies. Because of the missing high frequencies in the LES, both LES spectra at the 60- and 90-deg locations do not compare well against the experiment, although the LES with filtering only still produces an acceptable spectrum shape until a certain Strouhal number that is smaller than the experimental peak frequency. Note that the substantial noise overprediction, possibly due to the noisy inflow forcing, could influence the foregoing conclusions made from the analysis of the spectra comparisons. From a computational standpoint, an LES done using the DSM is 50% more time consuming than an LES done with filtering alone. It is hoped that the present work will be helpful toward a better understanding of the effect of SGS modeling on jet noise prediction.

Acknowledgments

This work was sponsored by the Indiana 21st Century Research and Technology Fund. The simulations presented in this Note were performed on the IBM-Corporation, Inc., scalable parallel research computer of Indiana University. We thank Phoi-Tack Lew for his help during the comparison of our large-eddy simulation spectra with the experiment.

References

[1]Visbal, M. R., and Rizzetta, D. P., "Large-Eddy Simulation on Curvilinear Grids Using Compact Differencing and Filtering Schemes," *Journal of Fluids Engineering*, Vol. 124, No. 4, 2002, pp. 836–847.

[2]Visbal, M. R., Morgan, P. E., and Rizzetta, D. P., "An Implicit LES Approach Based on High-Order Compact Differencing and Filtering Schemes (Invited)," AIAA Paper 2003-4098, June 2003.

[3]Bogey, C., and Bailly, C., "Effects on Inflow Conditions and Forcing on Subsonic Jet Flows and Noise," *AIAA Journal*, Vol. 43, No. 5, 2005, pp. 1000–1007.

[4]Bogey, C., and Bailly, C., "LES of a High Reynolds, High Subsonic Jet : Effects of the Subgrid Modellings on Flow and Noise," AIAA Paper 2003-3557, June 2003.

[5]Bogey, C., and Bailly, C., "Decrease of the Effective Reynolds Number with Eddy–Viscosity Subgrid-Scale Modeling," *AIAA Journal*, Vol. 43, No. 2, 2005, pp. 437–439.

[6]Moin, P., Squires, K., Cabot, W., and Lee, S., "A Dynamic Subgrid-Scale Model for Compressible Turbulence and Scalar Transport, *Physics of Fluids A*, Vol. 3, No. 11, 1991, pp. 2746–2757.

[7]Uzun, A., "3-D Large Eddy Simulation for Jet Aeroacoustics," Ph.D. Dissertation, School of Aeronautics and Astronautics, Purdue Univ., West Lafayette, IN, Dec. 2003.

[8]Lele, S. K., "Compact Finite Difference Schemes with Spectral-Like Resolution," *Journal of Computational Physics*, Vol. 103, No. 1, 1992, pp. 16–42.

[9]Visbal, M. R., and Gaitonde, D. V., "Very High-Order Spatially Implicit Schemes for Computational Acoustics on Curvilinear Meshes," *Journal of Computational Acoustics*, Vol. 9, No. 4, 2001, pp. 1259–1286.

[10]Bogey, C., and Bailly, C., "A Family of Low Dispersive and Low Dissipative Explicit Schemes for Flow and Noise Computations," *Journal of Computational Physics*, Vol. 194, No. 1, 2004, pp. 194–214.

[11]Uzun, A., Blaisdell, G. A., and Lyrintzis, A. S., "Application of Compact Schemes to Large Eddy Simulation of Turbulent Jets," *Journal of Scientific Computing*, Vol. 21, No. 3, 2004, pp. 283–319.

[12]Bogey, C., and Bailly, C., "Three-Dimensional Non-Reflective Boundary Conditions for Acoustic Simulations: Far Field Formulation and Validation Test Cases," *Acta Acustica*, Vol. 88, No. 4, 2002, pp. 463–471.

[13]Colonius, T., Lele, S. K., and Moin, P., "Boundary Conditions for Direct Computation of Aerodynamic Sound Generation," *AIAA Journal*, Vol. 31, No. 9, 1993, pp. 1574–1582.

[14]Bogey, C., Bailly, C., and Juvé, D., "Noise Investigation of a High Subsonic, Moderate Reynolds Number Jet Using a Compressible LES," *Theoretical and Computational Fluid Dynamics*, Vol. 16, No. 4, 2003, pp. 273–297.

[15]Uzun, A., Lyrintzis, A. S., and Blaisdell, G. A., "Coupling of Integral Acoustics Methods with LES for Jet Noise Prediction," *International Journal of Aeroacoustics*, Vol. 3, No. 4, 2005, pp. 1–50.

[16]Tanna, H. K., Dean, P. D., and Burin, R. H., "The Generation and Radiation of Supersonic Jet Noise. Vol. III, Turbulent Mixing Noise Data," U.S. Air Force Applied Physics Lab., Rept. AFAPL-TR-76-65-Vol. 3, Marietta, GA, Sept. 1976.

[17]Simonich, J., Narayanan, S., Barber, T. J., and Nishimura, M., "High Subsonic Jet Experiments Part 1: Aeroacoustic Characterization, Noise Reduction and Dimensional Scaling Effects," AIAA Paper 2000-2022, June 2000.

[18]Narayanan, S., Barber, T. J., and Polak, D. R., "High Subsonic Jet Experiments: Turbulence and Noise Generation Studies," *AIAA Journal*, Vol. 40, No. 3, 2002, pp. 430–437.

K. Ghia
Associate Editor